







SUPPLEMENTARY MATERIALS

Size and Magnetization Control of Magnetite NPs via Ethylene Glycol and Temperature for Ferrofluid and Magnetotargeting: Model Experiments

Artur A. Dzeranov^{1,2*}, Lyubov S. Bondarenko¹, Michail V. Prokofiev¹,
Roman A. Bondarenko³, Danil R. Abramov¹,
Gulzhian I. Dzhardimalieva^{1,2}, Kamila A. Kydralieva¹

¹Moscow Aviation Institute (National Research University), Moscow, Russia;

²Federal Research Center of Problems of Chemical Physics and Medicinal Chemistry, Chernogolovka, Russia;

³Institute of Applied Mechanics, Russian Academy of Sciences, Moscow, Russia

(*Corresponding author's e-mail: arturdzeranov99@gmail.com)

List of Content

Physico-chemical method for nanocomposite characterization (Figure S1).	S2
Crystal structure of nanoparticles (TEM).	S3
Schematic diagram of a flow-through setup for magnetotargeting experiments (Figure S2).	S4
Description of a flow-through setup for magnetotargeting experiments.	S5
Calculation of the magnetic field induction of a cylindrical magnet depending on the distance from the magnetite surface to the location of the nanoparticles.	S6
Calculation parameters for determining the induction at a distance from the magnet (Table S1).	S7
Magnetic field induction as a function of distance (Figure S3).	S8
Mathematical functions used to approximate experimental data (Table S2).	S9
The number of captured magnetite nanoparticles (Table S3).	S10
Approximation by mathematical functions of the curves of the dependence of the mass of captured particles on the mass of particles in the injection depending on the magnitude of the induction of the external magnetic field (Figure S4).	S11
Parameters for approximation of experimental values by mathematical functions (Table S4).	S12
Analysis of gravimetric data to determine the optimal fixed mass of magnetite nanoparticles on a magnet depending on the induction of an external magnetic field.	S13
Sigmoid models for describing the curves of the dependence of the mass of captured particles on the mass of particles in the injection (a) and the function of the mass fraction of collected particles on the mass of particles in the injection with extrema (b) for values of the induction of the external magnetic field (Figure S5).	S14
Parameters of sigmoid models and extrema on the graph of mass fractions of "captured" particles (Table S5).	S15

Transmission Electron Microscopy (TEM)

The morphological characteristics of the nanoparticles were studied using micrographs obtained on a JEOL JEM-1400 PLUS universal transmission electron microscope (JEOL, Akishima, Japan) at an accelerating voltage of 120 kV. All samples were suspended in distilled water using an ultrasonic processor (Fisherbrand, USA) at 75% amplitude until opalescence was achieved. Ten microliters of each suspension were applied to carbon-coated copper grids (200 mesh) pre-treated in a glow discharge cleaning system (PELCO Inc. USA). Based on the image analysis, particle size distribution histograms were constructed, and the electron diffraction data obtained in a selected area (electron diffraction patterns) were also analyzed. Particle sizes were calculated using ImageJ software, taking into account at least 100 particles per image. In addition, Selected Area Electron Diffraction (SAED) patterns were obtained with the TEM and then compared to reference patterns in the American Mineralogist Crystal Structure Database (AMCSD) for phase identification.

X-Ray Diffraction Analysis

The phase composition and primary particle size of the samples were determined by X-ray diffraction analysis (XRD) analysis using the Bragg-Brentano geometry on a Philips X'Pert diffractometer (Philips Analytical, Eindhoven, The Netherlands). Cu-K α radiation ($\lambda = 1.5406 \text{ \AA}$) was used as the X-ray source. The collected data were smoothed using the Savitzky-Golay algorithm. Measurements were performed at room temperature, covering an angular range of $10^\circ < 2\Theta < 110^\circ$ with a step size of 0.025° and a dwell time of 1 second per step. Particle size was determined using the Williamson-Hall method based on magnetite reflections and their widths at half maximum (WFWHM) in the Match!3 program. Lattice parameters for all samples were determined using the Rietveld method (Match!3 program).

Magnetic Properties

The magnetic properties of the samples were analyzed using an Oxford Instruments Vibrating Sample Magnetometer (VSM). The magnetic field induction ranged from -10,000 to +10,000 Oe at 25°C, allowing for the determination of saturation magnetization (σ_s), remanent magnetization (σ_r), and coercivity (H_c) for each sample.

Rheological Analysis of Nanofluid

Rheological analysis was carried out on the Rheostress RS150 (HAAKE, Germany) with cone-plane measurement unit, rotor angle 2 degrees, clearance 0.105 mm, rotor radius 35 mm in the range of shift deformations from 0.01 to 100 sec^{-1} . The temperature of the samples was between 36.6 and 40°C, controlled by a HAAKE DC50 thermal controller. The studies were carried out in a polyglucinum (PG) medium used as a plasma substitute, which is a 6% solution of an intramolecular fraction (50 kD) of hydrolyzed dextran with the addition of 0.9% NaCl.

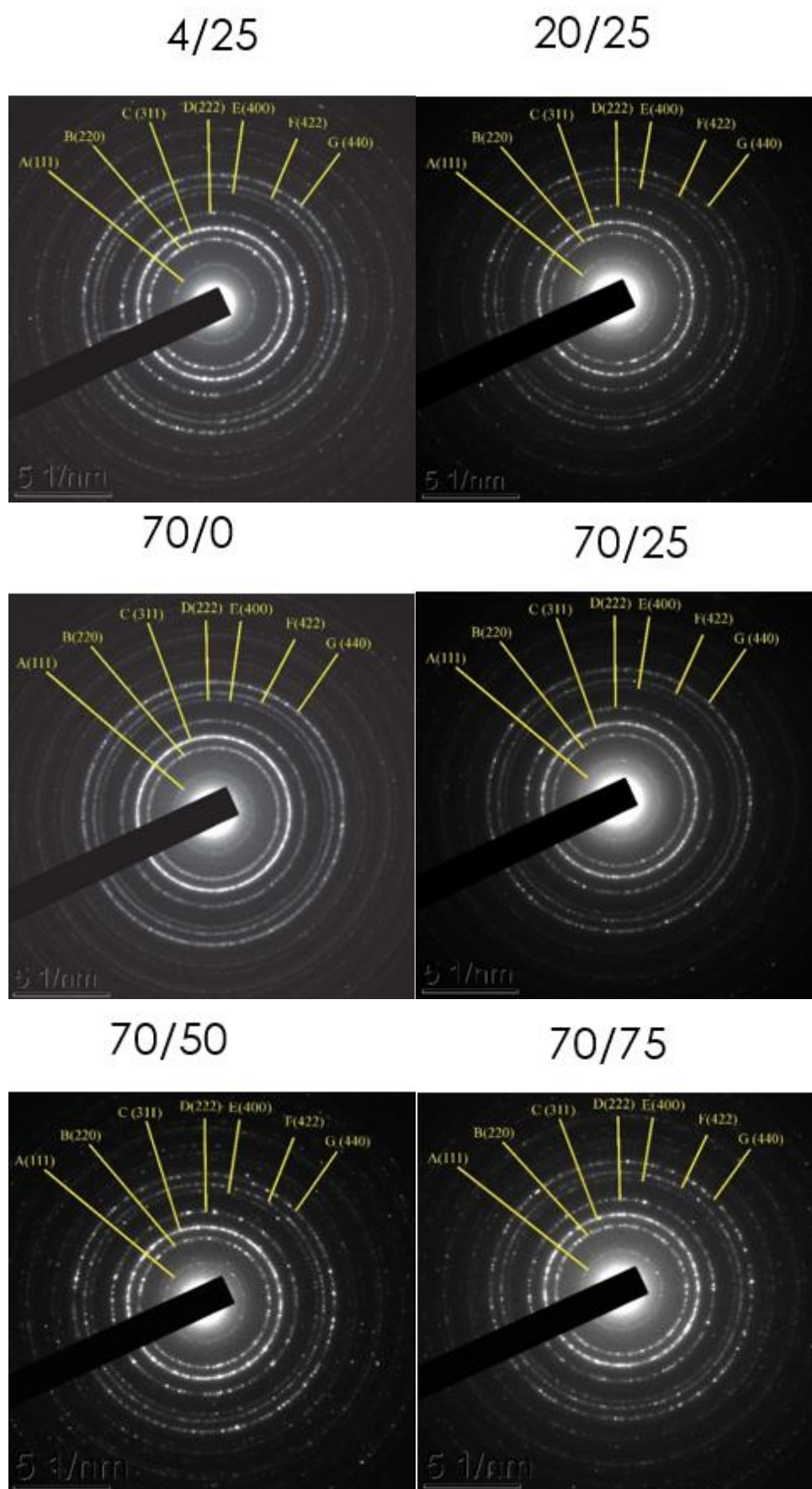


Figure S1. Electron diffraction results in a selected area of the samples. The numbers in brackets correspond to the hkl indices of the atomic planes

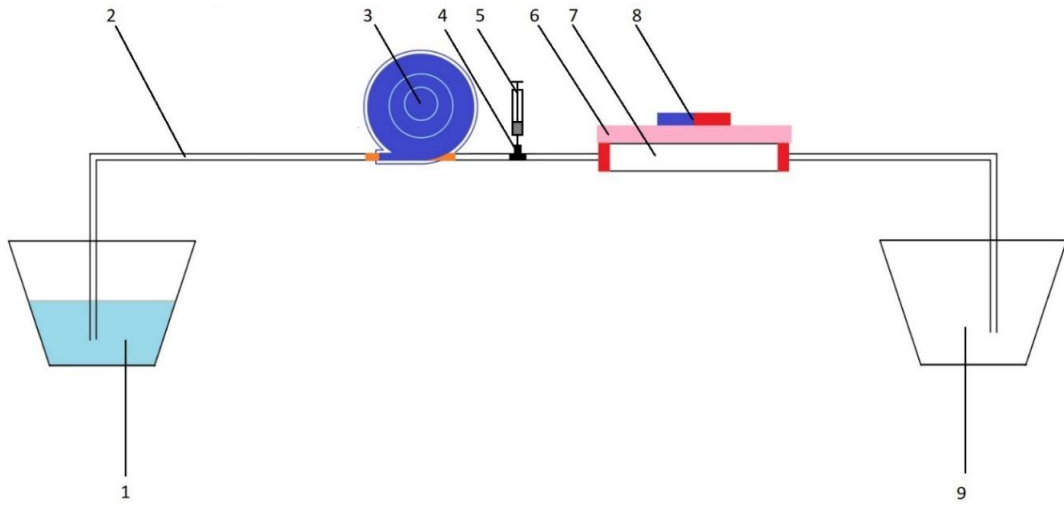


Figure S2. Scheme of a flow-through setup for magnetotargeting experiments

Description of a Flow-Through Setup for Magnetotargeting Experiments

To conduct sorption experiments for magnetotargeting of target magnetically active drugs, a specialized setup was developed. This system evaluates the retention efficiency of magnetite nanoparticles, which serve as model magnetically active drugs, under the influence of a magnetic field. The setup allows for studying the impact of various parameters on NPs retention, including magnetic field strength, distance to the magnet, the presence of biological tissue simulators, and fluid flow rate. The setup components are as follows:

1. **Medium Reservoir:** A plastic or glass vessel designed to store the medium (without NPs), featuring an outlet for introduction into the system.
2. **Tubing:** Silicone tubing (3 mm inner diameter, 5 mm outer diameter) connects the various system components. Its chemical resistance, hygienic properties, and transparency allow for visual monitoring of the fluid flow and suitability for a peristaltic pump.
3. **Peristaltic Pump:** This pump ensures continuous fluid flow through the system and features an adjustable flow rate. It establishes a linear flow velocity within the experimental tube with a target value of 9.5 mm/s.
4. **Tee Connector:** A device that connects two sections of tubing and provides an opening for the syringe, used to inject NPs into the flow.
5. **A magnetite Injection Syringe:** Utilized for direct injection of NPs into the fluid flow.
6. **Magnetite Sorption Tube Section:** This specific section of the silicone tube is where NPs capture occurs near the target.
7. **Magnetic System:** Comprises permanent neodymium magnets with a saturation induction of 1.3 T. These magnets are positioned at an adjustable distance (0 to 5 cm) from the experimental tube.
8. **Tissue Simulation Materials:** To simulate the attenuating effect of biological tissue on the magnetic field, chicken fillet is used for muscle tissue, and pork fat for skin and adipose tissue. These materials are placed between the magnet and the experimental tube.
9. **Collection Reservoir:** A plastic or glass vessel used to collect the fluid after it has passed through the entire system.

Calculation of the Magnetic Field Induction of a Cylindrical Magnet Depending on the Distance from the Magnetite Surface to the Location of the Nanoparticles

In this work, the following formula was used to calculate the magnetic field induction B on the axis of a cylindrical permanent magnet:

$$B = B_0 \cdot \frac{\cos \beta - \cos \alpha}{2}, \quad (1)$$

where B_0 is the residual induction of the magnet (the maximum field on its surface), α is the angle between the magnet axis and the line connecting the measurement point to the near edge of the magnet. β is the angle between the magnet axis and the line connecting the measurement point to the far edge of the magnet.

The formula is derived from the model of a cylindrical magnet as an equivalent solenoid with surface currents based on the Biot-Savart law and takes into account the magnet geometry (diameter and height) as well as the distance to the measurement point.

Formula (2) allows us to calculate the magnetic field induction (B) on the axis of a cylindrical magnet depending on the distance (r) from its surface:

$$\begin{aligned} B &= B_0 \cdot \frac{\cos \beta - \cos \alpha}{2} = B_0 \cdot \frac{\frac{r+h}{\sqrt{\left(\frac{d}{2}\right)^2 + (r+h)^2}} - \frac{r}{\sqrt{\left(\frac{d}{2}\right)^2 + r^2}}}{2} = \\ &= 1.3 \cdot \frac{\frac{r+0.020}{\sqrt{(0.025)^2 + (r+0.020)^2}} - \frac{r}{\sqrt{(0.025)^2 + r^2}}}{2}, \end{aligned} \quad (2)$$

where B_0 is the residual induction of the magnet. h is the height of the magnet. d is the diameter of the magnet.

Using formula (2), the inductions for each distance were calculated. The results are presented in Table S1 and a graphical representation of the approximated function is shown in Fig. S3.

Table S1

Calculation parameters for determining the induction at a distance from the magnet

Distance, cm	cosβ	cosα	B, T
0	0.624	0	0.40
0.5	0.707	0.196	0.33
1	0.768	0.371	0.25
2	0.847	0.624	0.14
3	0.894	0.768	0.08
5	0.941	0.894	0.03

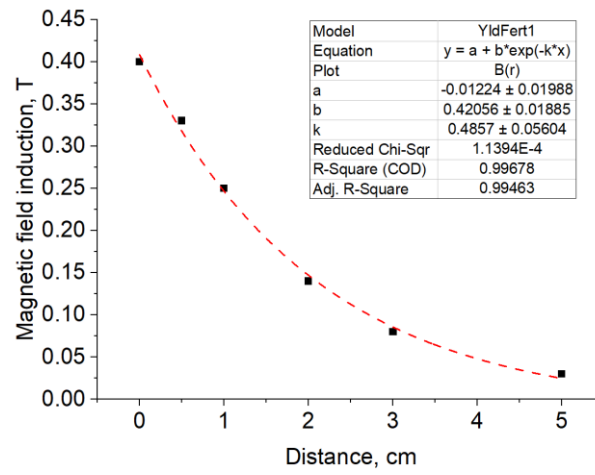


Figure S3. Magnetic field induction as a function of distance

Mathematical functions used to approximate experimental data

Equation	Note
<i>Power function</i>	
$f(x) = k \cdot x^n$	<p><i>Application:</i> Models processes with nonlinear growth/decay without saturation.</p> <p><i>Physical meaning:</i> Describes the initial portion of the dependence. where particle uptake increases as a power law. The parameter n characterizes the growth rate (slow for n<1, accelerated for n>1).</p> <p><i>Limitations:</i> Doesn't account for saturation. so it doesn't accurately describe data at large x values.</p>
<i>Exponential function</i>	
$f(x) = A \cdot (1 - e^{-k \cdot x})$	<p><i>Application:</i> Classical model of saturation processes.</p> <p><i>Physical meaning:</i> A is the limiting mass at infinite injection (capacity), k is the saturation rate (depends on the magnetic field strength).</p> <p><i>Advantages:</i> Well describes systems where growth slows with increasing x.</p>
<i>Rational function</i>	
$f(x) = \frac{k \cdot x}{1 + b \cdot x}$	<p><i>Application:</i> A special case of the Langmuir equation for adsorption.</p> <p><i>Physical meaning:</i> k/b is the limiting value as $x \rightarrow \infty$. 1/b is the characteristic mass at which the system reaches half saturation.</p> <p><i>Relation to experiment:</i> Can be interpreted as the ratio of the probability of particle capture to the probability of particle loss.</p>
<i>Sigmoid function</i>	
$f(x) = \frac{L}{1 + e^{-k \cdot (x-x_0)}}$	<p><i>Application:</i> Universal model for S-shaped dependencies.</p> <p><i>Physical meaning:</i></p> <p>L is saturation level;</p> <p>k is transition steepness (depends on the field induction);</p> <p>x_0 is inflection point (characteristic mass at half saturation).</p>

The number of captured magnetite nanoparticles

B, T	M*₁	M₂	M₃	M₄	M₅	M₆	M₇
0.40	0.010	0.020	0.050	0.060	0.094	0.106	0.110
0.33	0.009	0.017	0.046	0.059	0.091	0.104	0.110
0.25	0.006	0.014	0.029	0.042	0.058	0.064	0.065
0.14	0.004	0.012	0.026	0.035	0.048	0.050	0.056
0.08	0.002	0.007	0.014	0.018	0.024	0.026	0.030
0.03	0.001	0.003	0.006	0.007	0.009	0.009	0.012

* M_N is the mass collected as a result of fixing a magnet in the N experiment with mass m_N for a certain distance (g).

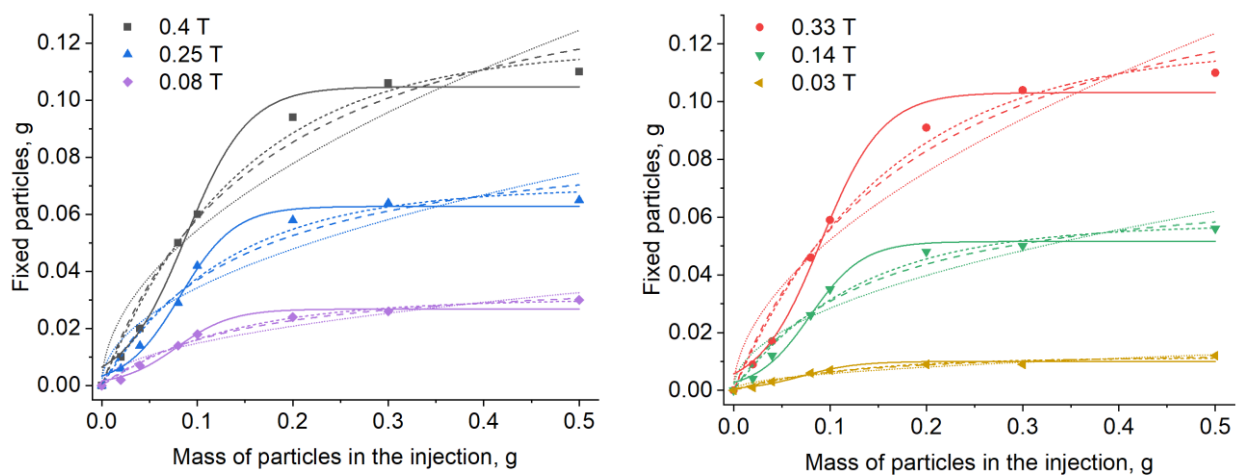


Figure S4. Approximation by mathematical functions of the curves of the dependence of the mass of captured particles on the mass of particles in the injection depending on the magnitude of the induction of the external magnetic field (0.03 – 0.4 T)

Parameters for approximation of experimental values by mathematical functions

Function	Parameter							
	k	n/A/b/L	x ₀	R ²	k	n/A/b/L	x ₀	R ²
B = 0.4 T					B = 0.14 T			
Power	0.12	0.5	-	0.926	0.09	0.5	-	0.919
Exponential	7	0.12	-	0.989	8	0.07	-	0.983
Rational	0.9	6	-	0.977	0.5	7	-	0.973
Sigmoid	31	0.19	0.09	0.989	37	0.05	0.08	0.989
B = 0.33 T					B = 0.08 T			
Power	0.18	0.5	-	0.928	0.05	0.5	-	0.937
Exponential	6	0.12	-	0.986	8	0.03	-	0.987
Rational	0.8	5	-	0.976	0.27	7	-	0.983
Sigmoid	31	0.10	0.09	0.987	35	0.027	0.09	0.975
B = 0.25 T					B = 0.03 T			
Power	0.10	0.5	-	0.908	0.017	0.5	-	0.942
Exponential	8	0.07	-	0.982	8	0.011	-	0.969
Rational	0.6	7	-	0.968	0.11	8	-	0.974
Sigmoid	34.9	0.06	0.08	0.992	36	0.010	0.07	0.944

Analysis of Gravimetric Data to Determine the Optimal Fixed Mass of Magnetite Nanoparticles on a Magnet Depending on the Induction of an External Magnetic Field

The combined sigmoid curve plot is shown in Fig. S5a. The injection mass at which the fraction of "captured" particles reaches its maximum corresponds to the injection mass at which the particle "capture" efficiency is maximized—this is the optimal injection mass for maximizing injection efficiency. Thus, the maximum efficiency from the injected mass will be achieved at this value.

Fig. S5b shows the extrema of the functions of the mass fraction of collected particles as a function of the particle mass in the injection. Table S5 presents the mass and mass fraction values for the extrema points at a given distance.

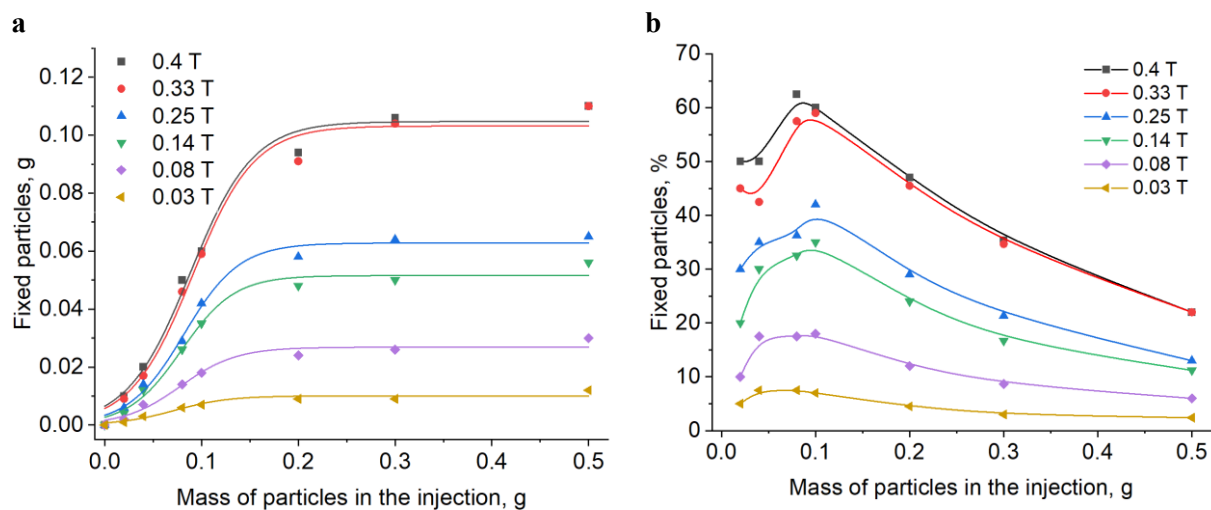


Figure S5. Sigmoid models for describing the curves of the dependence of the mass of captured particles on the mass of particles in the injection (a) and the function of the mass fraction of collected particles on the mass of particles in the injection with extrema (b) for values of the induction of the external magnetic field (0.03 – 0.4 T)

Table S5

Parameters of sigmoid models and extrema on the graph of mass fractions of "captured" particles

B, T	k	x_0	R^2	Mass fraction of "captured" particles, %
0.40	31	0.09	0.989	63.4
0.33	31	0.09	0.987	61.5
0.25	35	0.08	0.992	41.5
0.14	37	0.08	0.987	35.4
0.08	35	0.08	0.975	18.3
0.03	35	0.07	0.944	7.3